

Sub-shot-noise photon-number correlation in mesoscopic twin-beam of light

Maria Bondani,^{1,*} Alessia Allevi,² Guido Zambra,^{3,4} Matteo G. A. Paris,⁴ and Alessandra Andreoni²

¹National Laboratory for Ultrafast and Ultraintense Optical Science - C.N.R.-I.N.F.M., Como, Italy

²C.N.R.-I.N.F.M.-C.N.I.S.M., Dipartimento di Fisica e Matematica, Università dell'Insubria, Como, Italy

³Dipartimento di Fisica e Matematica, Università dell'Insubria, Como, Italy

⁴Dipartimento di Fisica dell'Università di Milano, Italy

(Dated: February 9, 2020)

We demonstrate sub-shot-noise photon-number correlations in a (temporal) multimode mesoscopic ($\sim 10^3$ detected photons) twin-beam produced by ps-pulsed spontaneous non-degenerate parametric downconversion. We have separately detected the signal and idler distributions of photons collected in twin coherence areas and found that the variance of the photon-count difference goes below the shot-noise limit by 3.25 dB. The number of temporal modes contained in the twin-beam, as well as the size of the twin coherence areas, depends on the pump intensity. Our scheme is based on spontaneous downconversion and thus does not suffer from limitations due to the finite gain of the parametric process. Twin-beams are also used to demonstrate the conditional preparation of a nonclassical (sub-Poissonian) state.

PACS numbers: 42.50.-p (quantum optics), 42.50.Dv (nonclassical states), 42.50.Ar (photon statistics and coherence theory), 42.65.Lm (Parametric down conversion and production of entangled photons)

The shot-noise limit (SNL) in any photodetection process is defined as the lowest level of noise that can be obtained by using semiclassical states of light, that is Glauber coherent states. If one measures the photon numbers of two beams and evaluates their difference, the SNL is the lower limit of the noise that can be reached when the beams are classically correlated. On the other hand, when intensity correlations below SNL are observed, we have a genuine quantum effect.

Quantum correlations between light beams play a crucial role in fundamental quantum optics [1] and find applications in quantum cryptography [2] and communication [3, 4], spectroscopy [5], interferometry [6], as well as in enhancing sensitivity in imaging [7] and high-precision measurements [8].

Quantum correlations have been the subject of intensive investigations and sub-shot-noise in photon-number correlations have been indeed observed through the generation of the so-called *twin-beam* of light. So far twin-beams have been obtained in the macroscopic regime from parametric oscillators [5, 9, 10] or from seeded parametric amplifiers [11, 12] and, with much lower photon numbers, from traveling-wave optical parametric amplifiers (OPA) [13, 14].

In this Letter we report what is, to our knowledge, the first demonstration of sub-shot-noise intensity correlations in a mesoscopic ($\sim 10^3$ detected photons) twin-beam obtained through spontaneous downconversion in a traveling-wave OPA not operated at frequency degeneracy. The scheme is conceptually simple: the signal and idler beams at the output of the amplifier are individually measured by direct detection. The resulting photon-counts, m_s and m_i , which are highly correlated, are subtracted from each other to demonstrate quantum noise reduction in the difference $d = m_s - m_i$. We calculate the variance of the difference, σ_d^2 , and show that

$$\sigma_d^2 < \langle m_s \rangle + \langle m_i \rangle,$$

where $\langle m_s \rangle$ and $\langle m_i \rangle$ are the average numbers of detected photons in the two output beams. The quantity $\langle m_s \rangle + \langle m_i \rangle$

is the SNL, *i.e.* the value of σ_d^2 that would be obtained for uncorrelated coherent beams.

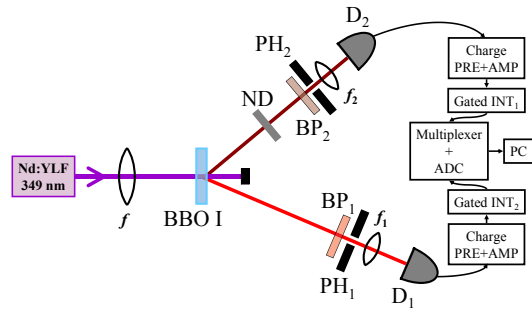


FIG. 1: Schematic diagram of the experimental setup. Nd:YLF, ps-pulsed laser source; BBO I, nonlinear crystal; f , $f_{1,2}$: converging lenses; $PH_{1,2}$, 100 μm diameter pin-holes; $D_{1,2}$, pin detectors; $BP_{1,2}$, band-pass filters; ND, variable neutral-density filter. The boxes on the right side of the figure indicate the parts of the signal amplification and acquisition chains.

The experimental setup is sketched in Fig. 1. A frequency-tripled continuous-wave (cw) mode-locked Nd:YLF laser regeneratively amplified at a repetition rate of 500 Hz (High Q Laser Production, Hohenems, Austria) produces linearly polarized pump pulses at 349 nm with pulse duration of 4.45 ps, as calculated from that of the fundamental pulse [15]. After passing through a 250-mm focal-length lens the pump beam comes to a focus (diameter $\sim 300 \mu\text{m}$) at the position where a 4-mm-thick uncoated $\beta\text{-BaB}_2\text{O}_4$ crystal (BBO I) is placed (Fujian Castech Crystals, Fuzhou, China). The crystal is cut for type I interaction at a 38.4-deg angle and it is adjusted to yield efficient parametric amplification of a cw He-Ne laser beam at 632.8 nm that hits the crystal at a 5.85-deg angle (external angle) to the pump beam. After the BBO I, at distances $d_1 = 60 \text{ cm}$ and $d_2 = 49 \text{ cm}$ respectively, two pin-holes of

100 μm diameter are positioned so as to be centered with the amplified signal beam at 632.8 nm and with the idler beam at 778.2 nm. The two different values chosen for the distances compensate the difference in the divergence of signal and idler related to their wavelengths. Stray light is blocked by two suitable band-pass filters, BP₁ and BP₂, placed before the pin-holes while the light transmitted by the pin-holes is conveyed to the detectors, D₁ and D₂, by two 25-mm focal-length lenses that are placed just beyond the pin-holes. The interaction seeded by the cw light at the signal wavelength is only used for the preliminary alignment of the pin-holes. The D₁ and D₂ detectors are pin photodiodes (S5973-02 and S3883, Hamamatsu Photonics K.K., Japan) with nominal quantum efficiencies of 86% and 90% at the signal and idler wavelengths, respectively. As the combinations of detectors and band-pass filters yield detection efficiencies of 55.0% in the signal arm and of 57.6% in the idler arm, the latter is lowered by adding an adjustable neutral-density filter, ND in Fig. 1, in order to obtain the same overall detection efficiency, $\eta = 0.55$, on both arms.

The current outputs of the detectors are amplified by means of low-noise charge-sensitive pre-amplifiers (CR-110, Cremat, Watertown, MA) followed by amplifiers (CR-200-4 μs , Cremat, Watertown, MA) which are identical in the two arms. The two amplified outputs are integrated over gates of 15 μs duration synchronized with the pump pulse by Gated INT_{1,2} in Fig. 1 (SR250, Stanford Research Systems, Palo Alto, CA). The voltage outputs are sampled, digitized and recorded by a computer. Accurate calibrations of the voltage outputs per electron in the detector current pulses give 33.087 $\mu\text{V}/\text{el}$ for D₁ and 24.803 $\mu\text{V}/\text{el}$ for D₂. All the data presented in this Letter are in units of electrons in the D₁ and D₂ output current pulses, thus corresponding to the number of photons detected in the signal and idler.

The size of the pin-holes and their distance from the crystal have been chosen so as to collect a single coherence area in the downconversion pattern. As the size of the coherence area depends on the pump intensity [16], we optimized the collection of the light by fixing distances and sizes of the pin-holes and by varying the pump intensity. The distributions of the detected photons collected by the pin-holes are temporally multimode [15]. In order to demonstrate that we selected twin coherence areas we plot in the Inset of Fig. 2 the detected photons of the signal (m_s) as a function of those of the idler (m_i) for $K = 10^5$ subsequent laser shots. At the pump intensity used in this measurement, the average number of detected photons were: $\langle m_s \rangle = 528$ and $\langle m_i \rangle = 593$. To emphasize the presence of correlations in the parties of the twin-beam we evaluated the correlation function

$$\Gamma(j) = \frac{\sum_{k=1}^K [(m_s(k) - \langle m_s \rangle) (m_i(k+j) - \langle m_i \rangle)]}{\sqrt{\sigma^2(m_s)\sigma^2(m_i)}}, \quad (1)$$

where j and k index the shots and $\sigma^2(m) = \langle m^2 \rangle - \langle m \rangle^2$ is the variance. Note that Eq. (1) must be corrected by taking into account the presence of noise, both in terms of possible

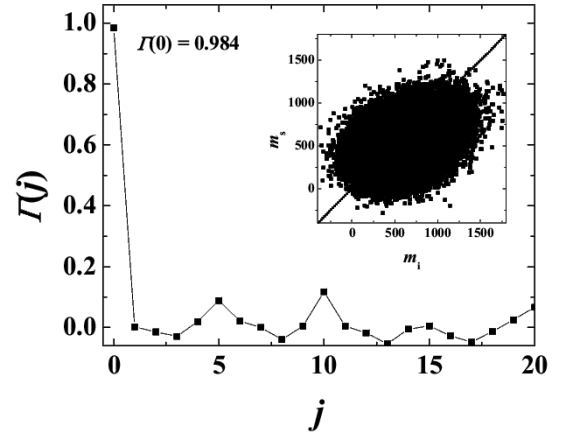


FIG. 2: Correlation function $\Gamma(j)$ as a function of the delay in the laser shots (index j numbers the shots). Inset: values of the photons detected in the signal as a function of those detected in the idler for the same laser shot.

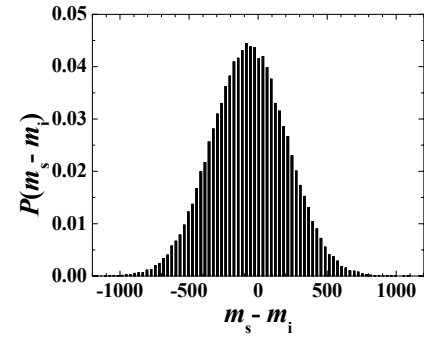


FIG. 3: Distribution of the difference photon-counts, $P(d)$, measured over 10^5 subsequent laser shots.

correlation and in terms of increased variance. In fact, typical values of the noise r.m.s. were $\sigma(m_{s,\text{dark}}) \sim 159$ and $\sigma(m_{i,\text{dark}}) \sim 214$. For the data in the inset, we obtained a value of the correlation coefficient $\Gamma(0) = 0.984$ that indicates a high degree of the correlation. As we emphasized in [17], a high value of correlation is not sufficient to discriminate between quantum and classical correlations since in both cases $\Gamma(0) \rightarrow 1$.

An explicit marker of nonclassicality can be obtained by considering the distribution of the photon-count difference $P(d)$, which is plotted in Fig. 3 for the same data displayed in the Inset of Fig. 2. The distribution appears symmetrical and centered at zero, which indicates both accurate balance of the overall efficiencies of the detectors and high correlation in signal/idler photon numbers. In order to assess the nonclassicality of the twin-beam, we calculate the quantum noise reduction R

$$R = \frac{\sigma_d^2}{\langle m_s + m_i \rangle}, \quad (2)$$

where, as in the case of the correlation function, the variance of the photon-count difference must be corrected for the electronic noise in the absence of light $\sigma_d^2 \rightarrow \sigma_d^2 - \sigma_{d,\text{dark}}^2$.

In principle, we have quantum noise reduction whenever the noise reduction falls in the range $0 < R < 1$ and the whole range is achievable. On the other hand, in order to assess quantitatively the quantum noise reduction, the overall detection efficiency η , which somewhat degrades the observed correlations, should be taken into account. By assuming that both arms of the measurement have the same efficiency and that dark counts have been already subtracted, the probability operator-valued measure (POVM) of each detector is given by a Bernoullian convolution of the ideal number operator spectral measure

$$\hat{\Pi}_{m_j} = \eta_j^{m_j} \sum_{n_j=m_j}^{\infty} (1 - \eta_j)^{n_j - m_j} \binom{n_j}{m_j} |n_j\rangle\langle n_j|, \quad (3)$$

with $j = s, i$. The joint distribution of detected photons $p(m_1, m_2)$ can be evaluated by tracing over the density matrix of the two modes, while the moments of the distribution are evaluated by means of the operators $\hat{m}_j^p = \sum_{m_j} m_j^p \hat{\Pi}_{m_j} = \sum_{n_j=0}^{\infty} (1 - \eta)^n G_{\eta_j}(n_j) |n_j\rangle\langle n_j|$ where $G_{\eta}(n) = \sum_{m=0}^n \binom{n}{m} \left(\frac{\eta}{1-\eta}\right)^m m^p$. Of course, since \hat{m}_j^p are operatorial moments of a POVM, we have, in general, $\widehat{m}_j^p \neq \hat{m}_j^p$. The first two moments correspond to the operators $\hat{m}_j = \eta_j \hat{n}_j$ and $\widehat{m}_j^2 = \eta_j^2 \hat{n}_j^2 + \eta_j(1 - \eta_j) \hat{n}_j$. As a consequence, the variances of the two photocurrents are larger than the corresponding photon number variances. We have $\sigma^2(m_j) = \eta_j^2 \sigma^2(n_j) + \eta_j(1 - \eta_j) \langle \hat{n}_j \rangle$. Using this relations we may evaluate the expected noise reduction, which, for our multimode twin-beam obtained by spontaneous down-conversion, is given by

$$R = 1 - \eta, \quad (4)$$

independently of the gain of the amplifier.

If $1 > R > (1 - \eta)$ the field displays nonclassical correlations [17], whereas $R = 1$ marks the boundary between classical and nonclassical behaviors. For the data in Fig. 2, which correspond to maximum noise reduction, we get a value $R = -3.25$ dB below SNL. Notice that given the overall detection efficiency $\eta = 55\%$ ($1 - \eta = -3.47$ dB), this is almost the maximum detectable noise reduction and corresponds to an ideal noise reduction (corrected for the quantum efficiency, *i.e.* measured by high-efficiency detectors at the output of the crystal) equal to $R = -14.4$ dB. Notice also that the use of spontaneous (not seeded) downconversion allows us to have a quantum noise reduction that is independent of the gain of the parametric amplifier. In fact, for an amplifier seeded by a coherent signal [11, 12] the noise reduction is expected to be

$$R = 1 - \eta \left(1 + \frac{1}{2|\nu|^2} \frac{|\alpha|^2}{1 + |\alpha|^2} \right)^{-1}, \quad (5)$$

where α is the amplitude of the coherent seed and $|\nu|^2$ is the gain of the OPA. For $\alpha \gg 1$ we have $R \simeq 1 - \eta + \eta/(2|\nu|^2)$ and sub-shot-noise correlations may be observed only for high-gain amplifiers.

The study of R as a function of the pump intensity represents an useful criterion for the selection of a single coherence area. To this aim, in Fig. 4 we show the values of R measured by keeping fixed the collection areas (same pin-holes located at the same distances as for the data in the previous figures) and by varying the intensity of the pumping beam. The figure shows that there is an optimum condition at which R is minimum. In fact, increasing the pump intensity leads to the enlargement of the coherence areas so that they are only partially transmitted by the pin-holes (values on the right side of Fig. 4 with respect to the minimum). On the contrary, lowering the pump intensity reduces the size of the coherence areas and hence introduces uncorrelated light in the pin-holes (values on the left side of Fig. 4 with respect to the minimum). Note that the values of R corresponding to the selection of more than a single coherence area remain below the SNL or quite close to it as the information contained in the twin areas is not lost, but only made more noisy. On the other hand, selecting only part of the areas causes a loss of information thus determining an abrupt increase of R above the SNL. We interpret this result as an indication of the need of perfect matching of the coherence areas with the pin-hole areas in order to obtain sub-shot noise correlations. Note that, as the detected twin-beam is dichromatic, errors in the positioning of the pin-holes do not affect the two parties of the twinbeam in the same way.

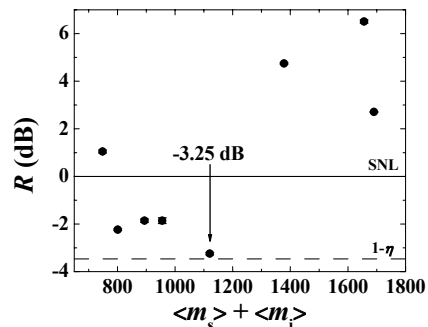


FIG. 4: Quantum noise reduction R (in units of dB) as a function of the average number of detected photons in the signal and idler beams. Solid and dashed lines denote the shot-noise level and the minimum value $R = 1 - \eta$ of the noise reduction, respectively. Error bars are within the size of the plotted points.

The results reported so far demonstrate the sub-shot-noise, *i.e.* quantum, nature of the intensity correlations in our twin-beam. These features should not be confused with the presence of entanglement, which, though expected in our system, cannot be claimed on the basis of the present measurements (a direct evidence of entanglement would be achievable by mea-

suring two conjugated quadratures by homodyne detection). Nonetheless, our system is suitable to generate mesoscopic single-beam nonclassical states by conditional measurements [18].

The conditional measurement is made as follows: the number of detected photons in the idler, m_i , is kept only if the number of detected photons in the signal, m_s , falls into a specific interval far from its mean value. The conditional distribution is reported in Fig. 5 together with the original unconditional distribution. The narrowing of the distribution below the SNL is apparent. The Fano factor ($F = \sigma^2(m)/\langle m \rangle$) of the idler conditional distribution, suitably corrected for the noise, is given by $F_c = 0.062$ (to be compared to that of the original unconditional marginal distribution $F = 28.95$), which corresponds to a noise reduction of about 12 dB below the single-beam shot-noise level. The probability of success, *i.e.* the fraction of data that are kept to build the distribution is 0.22%. The success probability may be increased by enlarging the interval of acceptance, at the price of increasing the Fano factor, which goes above unity if the acceptance window is too large or closer to the mean value of the unconditional distribution [18].

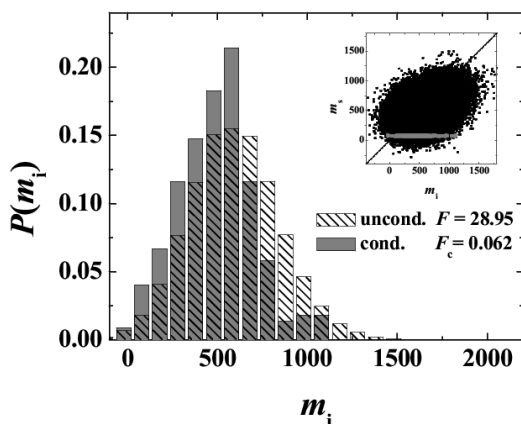


FIG. 5: Unconditional marginal distribution for the idler and conditional distribution obtained upon selecting the data marked in gray in the inset.

Our detection scheme, being based on direct detection of the photons in the two arms of the twin-beam, is somehow more noisy than those adopted in [11, 12], that make use of electronic subtraction of the pin photocurrents of signal and idler. On the other hand, our technique has the advantage of keeping the information about the marginal probability distributions, whose data can be used for state conditioning/engineering by post-selection on one of the two parties. Of course, when the information on the marginal distributions is not required, the direct measurement of the difference photocurrent is preferable. Our technique, being based on the ability of properly selecting the twin coher-

ence areas, provides a system suitable for many applications exploiting the sub-shot-noise correlations of the twin-beam [19, 20, 21, 22, 23]. Indeed, the twin-beam may be used as a maximally effective probe to reveal either tiny displacements imposed by light-matter interactions or by external perturbations. For instance, one can implement absorption measurements of weakly absorbing samples by looking at the degradation of the noise reduction or at the variation of the Fano factor in conditional measurements, thus improving the performances of single-mode techniques [24]. In this framework, the fact that the twin-beam is dichromatic, and hence its two parties are tunable in frequency, is undoubtedly relevant.

In conclusion, we have demonstrated the possibility of obtaining sub-shot-noise intensity correlations in the ps-pulsed mesoscopic regime by properly selecting the twin coherence areas on the parties of the twin-beam. Our system, which is based on spontaneous downconversion, does not suffer from limitations due to the finite gain of the parametric process and allows us to demonstrate conditional generation of sub-Poissonian light. The mesoscopic nature of our twin-beams makes them a promising system to reveal the presence of small perturbations, *e.g.* weakly absorbing biological samples, in a non-destructive illumination regime suitable to preserve even photolabile compounds.

This work has been supported by MIUR projects PRIN-2005024254-002 and FIRB-RBAU014CLC-002.

* Electronic address: maria.bondani@uninsubria.it

- [1] M. Bondani et al., *Opt. Lett.* **29**, 180 (2004).
- [2] A. C. Funk and M. G. Raymer, *Phys. Rev. A* **65**, 042307 (2002).
- [3] A. Porzio et al., *Opt. Laser Eng.*, in press.
- [4] V. C. Usenko and M. G. A. Paris, preprint quant-ph/0612028.
- [5] C. Schwob et al., *Opt. Lett.* **22**, 1893 (1997).
- [6] G. M. D'Ariano et al., *Phys. Rev. A* **65**, 062106 (2002).
- [7] N. Treps et al., *Phys. Rev. Lett.* **88**, 203601 (2002); A. F. Abouraddy et al., *Phys. Rev. Lett.* **93**, 213903 (2004).
- [8] T. Kim et al., *Phys. Rev. A* **72**, 055801 (2005).
- [9] A. Heidmann et al., *Phys. Rev. Lett.* **59**, 2555 (1987).
- [10] J. Gao et al., *Opt. Lett.* **23**, 870 (1998).
- [11] O. Aytür and P. Kumar, *Phys. Rev. Lett.* **65**, 1551 (1990).
- [12] D. T. Smithey et al., *Phys. Rev. Lett.* **69**, 2650 (1992).
- [13] M. Vasilyev et al., *Phys. Rev. Lett.* **84**, 2354 (2000).
- [14] O. Jedrkiewicz et al., *Phys. Rev. Lett.* **93**, 243601 (2004).
- [15] F. Paleari et al., *Opt. Express* **12**, 2816 (2004).
- [16] A. Allevi et al., *Laser Physics* **16**, 1451 (2006).
- [17] A. Agliati et al., *J. Opt. B* **7**, S652 (2005).
- [18] J. Laurat et al., *Phys. Rev. Lett.* **91**, 213601 (2003).
- [19] A. S. Lane et al., *Phys. Rev. A* **38**, 788 (1988).
- [20] P. R. Tapster et al., *Phys. Rev. A* **44**, 3266 (1991).
- [21] C. D. Nabors et al., *Phys. Rev. A* **42**, 556 (1990).
- [22] J. J. Snyder et al., *J. Opt. Soc. Am. B* **7**, 2132 (1990).
- [23] A. Porzio et al., *Appl. Phys. B* **73**, 763 (2001).
- [24] V. D'Auria et al., *J. Phys. B* **39**, 1187 (2006).